PREPARATION AND CHARACTERIZATION OF POLY(ACRYLONITRILE-CO-VINYL ACETATE) HOLLOW FIBER MEMBRANES FOR WASTEWATER TREATMENT

Cite this: *INEOS OPEN*, **2025**, *8 (1–3)*, XX–XX
DOI: 10.32931/ioXXXXx

Received XX Month 20XX,
Accepted 25 January 2025

http://ineosopen.org

M. Shirzadkhan and M. Nouri*

Department of Textile Engineering, Faculty of Engineering, University of Guilan, Rasht, Iran

Abstract

The hollow fiber membranes of poly(acrylonitrile-co-vinyl acetate) were fabricated by the dry jet wet spinning method and used as membranes to separate disperse dyes from an aqueous solution. The effect of the coagulant on the mechanical properties of the hollow fibers and dye removal were investigated. The morphology and porosity of the hollow fibers were determined. The results showed that the addition of a solvent to the coagulants leads to a decrease in the permeability. The tensile strength of the membranes increased with an increase in the amount of a solvent in the coagulant. The hollow fibers spun with a higher solvent content showed lower hydraulic permeability and higher dye removal efficiency.

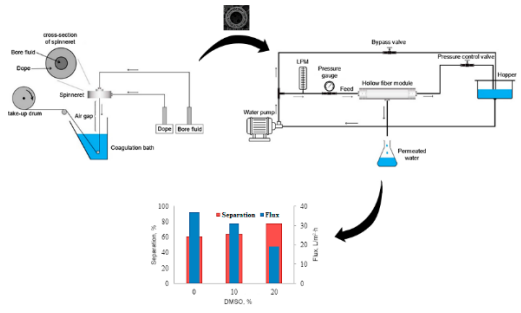

Key words: membrane, hollow fiber, disperse dye, wastewater, poly(acrylonitrile-co-vinyl acetate).

Introduction

Owing to an increase in the industrial activities, especially in the textile industry, water pollution issues have become the main concern of societies. Disperse dyes are among the dyes that are commonly used in dyeing processes and are known as dangerous pollutants for the environment. Purification and cleaning of textile effluents are necessary to prevent the spread of pollution and preserve water resources. In this regard, the use of membranes as an advanced and efficient technology enables the separation and removal of dyes effectively [1, 2]. Commercial separation methods like distillation and adsorption often require chemical additives and complex processes. Distillation uses heat to separate the components based on boiling points, while adsorption involves the use of materials like activated carbon to attract and hold specific molecules. In contrast, hollow fiber membranes achieve efficient separation with their high surface area-to-volume ratio, without the need for added chemicals, and offer more advantages than other methods, including improved separation performance, reduced costs, and higher efficiency. To increase the efficiency and capability of the hollow fiber membrane, many research efforts have been directed to improve the mechanical properties, morphology, and performance of the membrane by changing the spinning conditions [3–5]. While studying the effect of a stretch ratio on the properties of a polyacrylonitrile membrane, it was observed that the pore diameter increases with an increase in the stretch ratio of fibers. Moreover, the tensile strength and modulus reach 3.37 and 85.82 cN/dtex, respectively, when the draw ratio increase to 6 [6]. In another research conducted by Ahmed *et al.* [7], the influence of spinning conditions on the morphology and properties of hollow fibers was comprehensively investigated, and all factors, including the design of the spinneret, composition of the coagulation bath, temperature and flow rate of the spinning dope were discussed. The goal of this work was to prepare and characterize polyacrylonitrile-based hollow fiber membranes in order to separate disperse dyes from an aqueous solution and real textile effluent by examining the structure and functional characteristics of these membranes.

Results and discussion

Morphology and porosity of the hollow fiber membranes

Figure 1 shows the FE-SEM photomicrographs of the cross-section of the fabricated hollow fiber membranes. This figure

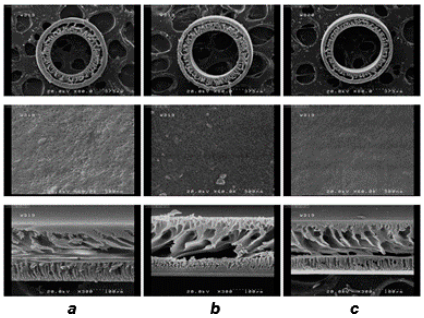

Figure 1. FE-SEM images of the cross-section and outer surface of the hollow fiber membranes: the fibers prepared in the water coagulant (***a***), fibers prepared in the coagulant containing 10% of DMSO (***b***), fibers prepared in the coagulant containing 20% of DMSO (***c***).

reveals an asymmetric structure of the membranes in which the outer dense layer has a greater thickness than the inner dense layer. This can be explained by the fact that the inner deposition of the fibers occurs immediately after exiting the spinneret due to a contact with the internal coagulant. In contrast, after a significant distance of air gap (15 cm), the fibers enter the external coagulant, where the external dense layer of the membrane is formed. Considering the diameter of the fibers and the presence of the dense inner layer, the preferred configuration for separation using these fibers is as follows: the fluid flow circulates through the inner lumen of the hollow fiber membrane, while the permeation flow occurs through the shell side. To investigate the effect of the coagulant composition on the morphology, Fig. 1 compares the samples in the left column (***a***), which were prepared in water coagulations, with the samples in the right column (***c***), which were obtained using a coagulant containing 20% of dimethyl sulfoxide (DMSO). It can be observed that the addition of 20% of DMSO to both the internal and external coagulants reduced the size of pores in the middle porous layer and dense layers, while increasing the number of pores in the outer dense layer. This modification may reduce the flux passing through the membrane and enhance its separation capabilities. By adding the solvent to the coagulation bath, a phase separation is delayed, allowing for a reduction in the porosity and size of the finger-like pores in the membrane structure.

Based on equation 3 (see the Experimental section), the percentage of fiber membrane porosity was calculated. According to the results shown in Fig. 2, by adding DMSO to the coagulants, the rate of non-solvent penetration decreased, and this caused a decrease in the size of finger-like pores in the middle layer and a decrease in the size of pores in the inner and outer dense layers. It can be seen that in all the resulting samples, the membrane porosity decreased upon addition of the solvent to the internal and external coagulant baths.

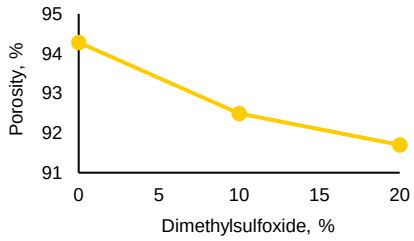

Figure 2. Porosity percentage diagram compared to DMSO being present in the coagulants according to the liquid permeation method.

Fourier-transform infrared spectroscopy

The FTIR spectroscopic studies were performed on a Nikolet Magna-IR 560 spectrophotometer (USA) in the range of 400–4000 cm^{-1}. Figure 3 shows the FTIR spectrum of the poly(acrylonitrile-co-vinyl acetate) powder in use. The absorption bands at 1820–1650 cm^{-1} can be attributed to the carbonyl group (C=O). The broad bands at 1629 and 1739 cm^{-1} correspond to the stretching vibrations of the carbonyl group in the acid and ester comonomers used for the synthesis of polyacrylonitrile. Strong absorption bands at *ca.* 1000–1300 cm^{-1} refer to the C–O group of the acetate unit, and the absorption band at 1237 cm^{-1} relates to the C–O bond. A characteristic signal of polyacrylonitrile is a strong and sharp band of the C≡N bond in the range of 2000–2500 cm^{-1} and, more precisely, at 2240–2260 cm^{-1}. This peak appeared at 2244 cm^{-1}. The region from 2850 to 3000 cm^{-1} is typical for the alkane C–H stretches. This band appeared at 2937 cm^{-1}. In the range of 1375–1450 cm^{-1}, the bending vibrations of CH_3 units were manifested as medium-intensity peaks. Two absorption bands at 1370 and 1451 cm^{-1} appeared in this region [8]. A broad band at *ca.* 3500 cm^{-1} can be attributed to water adsorbed by the polymer.

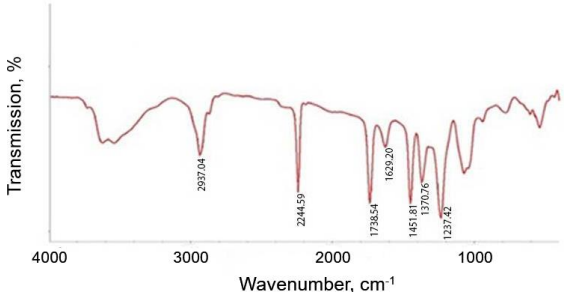

Figure 3: FTIR spectrum of poly(acrylonitrile-co-vinyl acetate).

Contact angle of the membranes

Polyacrylonitrile has a carbon–carbon main chain which is inherently non-polar and hydrophobic. Each repeating unit contains a nitrile group attached to the main chain. Owing to the electronegativity of the nitrogen atom and presence of the triple bond, nitrile groups can interact with polar solvents through polar bonding. However, the polymer is generally considered hydrophobic because the main chain largely determines its properties. In the case of poly(acrylonitrile-co-vinyl acetate), containing both acrylonitrile (C≡N) and acetate units, the acetate groups are also present along with the nitrile groups. These acetate groups (OC(O)Me) can enhance the hydrophilicity of the copolymer by increasing its surface energy. Compared to neat polyacrylonitrile, the copolymer is more hydrophilic due to the presence of acetate groups, implying that the higher content of the vinyl acetate units, the more hydrophilic the copolymer becomes (Fig. 4).

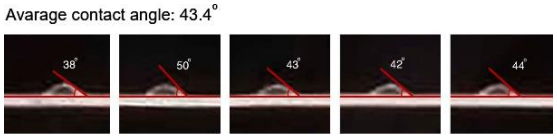

Figure 4: Contact angle of water droplets with the external surface of the hollow fibers of poly(acrylonitrile-co-vinyl acetate).

Mechanical properties of the hollow fiber membranes

Figure 5 shows the tensile strength and elongation at break of the hollow fibers obtained using different percentages of the solvent in the coagulants. As the amount of the solvent increases up to 20 vol % of the coagulants, the rate of the polymer enrichment decreases, resulting in an increase in the strength of the produced membrane from 9.0 to 10.2 (MPa). One of the most important parameters in the spinning process is the stability of the process and the prevention of membrane rupture during production and throughout the separation process. As it

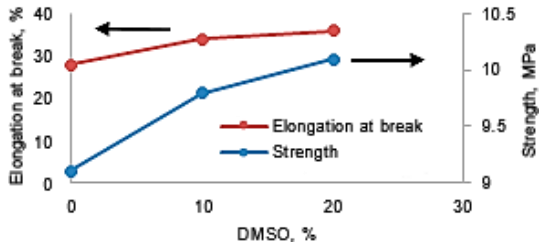

Figure 5: Strength and elongation at break of the hollow fiber membranes *obtained using* different amounts of the solvent in the coagulants.

was shown, an increase in the amount of the solvent leads to an increase in the elongation at break. This increase may be attributed to a decrease in the porosity of the fibers at higher contents of the solvent. A reduction of the spongy structure and porosity of the membrane leads to an increase in the elongation at break of the fibers.

Permeability and disperse dye separation

The hydraulic permeability of the resulting membranes was calculated (Fig. 6). As can be seen, the permeability of the membrane in the case where there is no solvent in the coagulation bath and the internal coagulant at the same pressure is higher than that of the membrane prepared upon addition of the coagulant. This indicates easy passage of the solution in the absence of a solvent in the coagulant. Figure 7 shows the separation percentage of the dye Disperse blue 165 compared to the flux through the coagulated hollow fiber membrane in different coagulation baths. An increase in the amount of DMSO in the coagulation bath leads to a decrease in the percentage of separation and removal of the disperse dye by the membrane, which is justified by a reduction in the percentage of porosity and the pore sizes. According to this graph, the polyacrylonitrile fibers obtained in the coagulation bath containing 20% of DMSO have the highest percentage of separation, but due to hydraulic permeability and low flux, the speed and efficiency of separation decreases. The separation percentage for the fibers coagulated without addition of a solvent was 61%, whereas the addition of 20% of the solvent led to an increase in the separation percentage to 78%. However, the flux passing through the membrane decreased to 19 (L/m²h) with the addition of 20% of the solvent, due to a reduction in the porosity and a decrease in the pore sizes of the dense surfaces. Therefore, to improve the efficiency while keeping the highest percentage of separation, further modifications of the membrane structure are required.

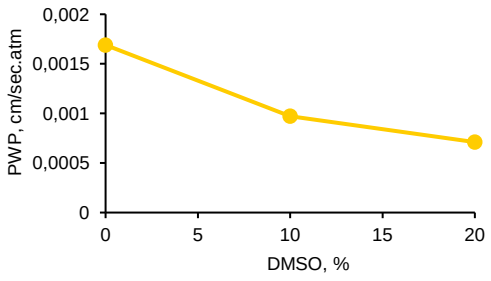

Figure 6: Permeability of the poly(acrylonitrile-co-vinyl acetate) hollow fiber membranes prepared in the coagulation bath containing different amounts of DMSO at 1.25 bar.

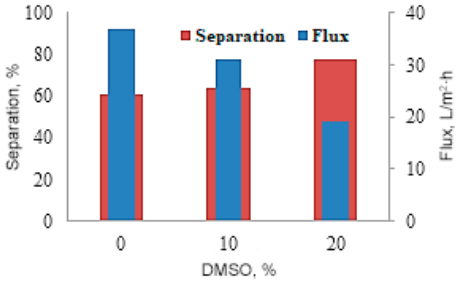

Figure 7: Separation and flux of the poly(acrylonitrile-co-vinyl acetate) hollow fibers obtained using different percentages of the solvent in the coagulants.

Experimental section

Materials

Poly(acrylonitrile-co-vinyl acetate) with a density of 1.184 g/mL and an average molecular weight of 70000, containing 6% of the vinyl acetate comonomer (for the chemical structure, see Fig. 8a), was purchased from Iranian Polyacrylic Factory. Dimethyl sulfoxide with a purity of 99.9% and a density of 1.096–1.106 g/mL at 20 °C was purchased from Spanish Carlo Erba Company. Disperse dye Terasil Blue BG (Diseprse blue 165) with a molecular weight of 405 g/mol was obtained from Ciba Specialized Chemical Products Company in Switzerland (for the chemical structure, see Fig. 8b).

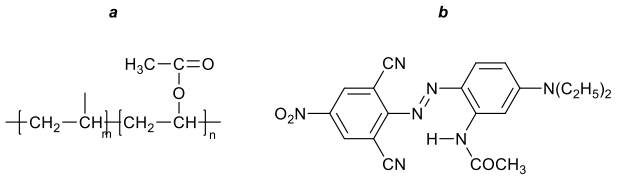

Figure 8: Chemical structures of poly(acrylonitrile-co-vinyl acetate) (***a***) and Disperse Blue 165 dye (***b***).

Spinning and preparation of the hollow fiber membrane module

The dry jet wet spinning machine consists of two main tanks for the passage of spinning dope and non-solvent, connection pipes, spinneret, coagulation bath, and take-up drum (Fig. 9). The spinneret used in this research has a tube-in-orifice nozzle structure with an inner diameter of 640 µm and an outside diameter of 1000 µm. The air gap was considered to be 15 cm, and spinning was carried out at an ambient temperature. The exit rate of the spinning solution was about 1 mL/min. The produced fibers were kept in distilled water for 24 h to completely remove remaining solvent, then they were dried at room temperature for 3 h.

The system depicted in Fig. 10 was used to assess the permeability and separation of the disperse dye by the prepared hollow fiber membranes. In this system, there is a place for the hollow fiber membrane module. The mentioned module was designed and made using a combination of glass and aluminum metal. 30 fibers were placed inside it and its two sides were completely sealed with an epoxy resin and it was left for 24 h to dry completely. It should be noted that new modules were prepared for each test.

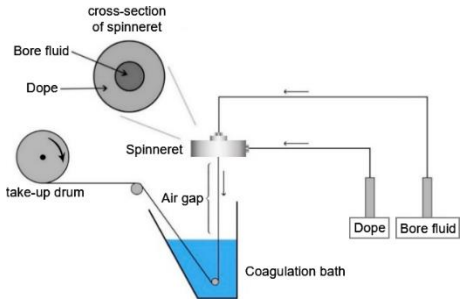

Figure 9: Schematic diagram of the used dry jet wet spinning apparatus.

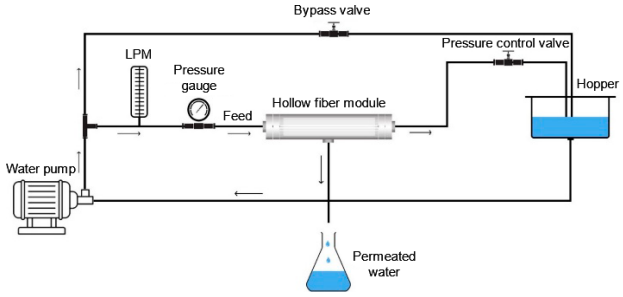

Figure 10: Schematic view of the experimental setup for measuring permeability of the hollow fibers.

Measurement of contact angle

The static contact angle between liquids and the hollow fiber surface was measured using the sessile drop method. For this purpose, a 4 µL droplet of the liquid was placed on the hollow fiber membrane surface. After capturing an image of the droplet's shape on the membrane, the contact angle was calculated through image processing. For each sample, at least 5 images of droplets were prepared and the average contact angle is reported.

Morphology and mechanical properties

The morphology of the cross-section of the poly(acrylonitrile-co-vinyl acetate) hollow fiber membranes was investigated using a Hitachi S4160 Field Emission Scanning Electron Microscope manufactured by Cold Field Emission Company. To examine the changes in the inner and outer diameters of the fibers, a Japanese Nikon XN stereo microscope was utilized, and the images were analyzed using the Digimizer software.

The measurements of tensile strength and elongation at break were conducted using a tensile tester (Shirley Testometric-Micro 50 apparatus, England). The machine operated at a speed of 10 mm/min, with a jaws distance of 10 mm. A minimum of 10 measurements were taken for each sample, and the average is reported. After determining the breaking force of the samples, the stress at the breaking point (σ_a) was calculated using equation 1.

$$\sigma_a = \frac{4F}{\pi(D^2 - d^2)} \quad (1)$$

where F is the breaking force, D is the outer diameter, and d is the inner diameter of hollow fibers.

The elongation at break of the fibers (ε) was calculated using equation 2.

$$\varepsilon = \frac{\Delta L}{L_0} \quad (2)$$

where ΔL is the elongation ratio and L_0 is the initial length of the fibers [9].

Determination of porosity

The porosity of the membranes was investigated using the liquid penetration method. In this procedure, the hollow fibers were first cut to a length of 5 cm and subsequently kept in a vacuum oven at 25 °C for 24 h. After drying, the fibers were weighed and then submerged in distilled water at 25 °C for additional 24 h. Following this immersion, the fibers were weighed again, after removing surface moisture with a paper filter. The porosity percentage (ε) was then calculated using equation 3.

$$\varepsilon = \frac{(w_1 - w_2)/\rho_w}{(w_1 - w_2)/\rho_w + w_2/\rho_p} \times 100 \quad (3)$$

where w_1 is the weight of the wet fiber, w_2 is the weight of the dry membrane, ρ_w is the water density, and ρ_p is the polymer density.

Permeability and separation properties of the hollow fiber membranes

Using the designed lab-scale setup (Fig. 10) and measuring the volume and time of permeation, the permeability and flux of the prepared hollow fiber membranes were evaluated. Equation 4 was used to calculate the hydraulic permeability.

$$L_p = \frac{Q}{A\,\Delta P} = \frac{Q}{n\,\pi\,d\,L\,\Delta P} \quad (4)$$

where Q is the volumetric flow rate (mL/min), A is the surface area of the hollow fiber membrane, n, d, and L are the number of fibers, the inner diameter of the hollow fibers, and the length of the hollow fibers, respectively, and ΔP is the membrane pressure in the test [10].

In order to check the separation rate of the disperse dye from the real effluent, it is necessary to prepare an initial solution similar to the effluent of industrial units so that we can accurately evaluate the ability of the produced hollow fiber membrane. For this purpose, a dyeing experiment was designed at high temperature and Disperse Blue 165 was used to dye polyester fabric with an L:R ratio of 1:40 and dyeing percentages of 0.05, 0.1, 0.5, 1, and 2. Furthermore, 10% acetic acid solution was used to adjust the pH value. After the dyeing process, the dye present in the effluent was mixed with acetone at a ratio of 1:1, and the absorbance was measured at the wavelength of 614 nm using a GBC UV-Visible Cintra 10 spectrophotometer (Varian, Australia). Finally, by using the calibration curve, the amount of dye present in the effluent (g/L) was determined and the concentration of the dye present in the actual effluent was obtained. Then, as mentioned earlier, the dye separation was measured using the designed system and the amount of the dye removal was calculated using equation 5.

$$R\% = 1 - \frac{C_p}{C_f} \quad (5)$$

where R is the separation rate, C_p and C_f are the dye concentrations in the permeate and in the feed solution, respectively [10].

Conclusions

Focusing on the discovery of new and optimal solutions in the field of textile wastewater treatment, in this study, we prepared the polyacrylonitrile-based hollow fiber membranes by the dry jet wet spinning method in different spinning conditions. By changing the composition of the external coagulation bath and internal coagulant using 0, 10, and 20 vol % of DMSO in distilled water, the fibers with different properties were produced to achieve the optimal conditions in membrane performance. The membrane porosity was calculated by the liquid permeation method. According to the FE-SEM analysis of the hollow fiber membranes, the surface of their selective layer has the pores of nano dimensions, and an increase in the amount of the solvent in the coagulants generally led to a decrease in the porosity of the membrane. Based on these results, it can be stated that the rate of exchange and movement of a solvent and non-solvent or the rate of enrichment of the polymer solution affected by the phase inversion from the non-solvent has a direct relationship with the porosity of the resulting membrane. Therefore, by adding DMSO to the coagulants, the rate of penetration of the non-solvent decreased. The results showed a decrease in the porosity with an increase in the percentage of DMSO, and at the DMSO content of 20 vol %, the separation percentage reached 78%.

Corresponding author

* E-mail: mnouri69@guilan.ac.ir. Tel: +98(912)310-0280 (M. Nouri).

References

1. R. Naim, G. P. Sean, Z. Nasir, N. M. Mokhtar, N. A. S. Muhammad, *Membrane*, **2021**, *11*, 839. DOI: 10.3390/membranes11110839
2. R. W. Baker, *Membrane Technology and Applications*, *2nd ed*., Wiley, Chichester, **2004**, ch. 1, pp. 1–14. ISBN 9780470020388
3. Z. Song, M. Xing, J. Zhang, B. Li, Sh. Wang, *Sep. Purif. Technol.*, **2012**, *90*, 221–230. DOI: 10.1016/j.seppur.2012.02.043
4. M. Pagliero, M. Khayet, C. García-Payo, L. García-Fernández, *Desalination*, **2021**, *516*, 115235. DOI: 10.1016/j.desal.2021.115235
5. M. Mulder, *Basic Principles of Membrane Technology*, Springer, Dordrecht, **1996**. DOI: 10.1007/978-94-009-1766-8
6. B. Zhang, C. Lu, Y. Liu, P. Zhou, Z. Yu, S. Yuan, *Polymer*, **2019**, *179*, 121618. DOI: 10.1016/j.polymer.2019.121618
7. A. L. Ahmed, T. A. Otitoju, B. S. Ooi, *J. Ind. Eng. Chem.*, **2019**, *70*, 35–50. DOI: 10.1016/j.jiec.2018.10.005
8. D. L. Pavia, G. M. Lampman, G. S. Kriz, J. R. Vyvyan, *Introduction to Spectroscopy*, Cengage Learning, **2015**.
9. W. L. Chou, D. G. Yu, M. C. Yang, *J. Polym. Res.*, **2005**, *12*, 219–229. DOI: 10.1007/s10965-004-3205-8
10. W. Fang, L. Shi, R. Wang, *J. Membr. Sci.*, **2013**, *430*, 129–139. DOI: 10.1016/j.memsci.2012.12.011